Proceedings of Science and Mathematics
Faculty of science, universiti teknologi malaysia
https://science.utm.my/procscimath
Volume 21 (2024) 40-50

Solute Dispersion in Casson Flow of Blood through a Stenosed Artery with Rigid Permeable Wall

Deserley Eric Marcus Dompok, Nurul Aini Jaafar*
Department of Mathematical Sciences, Faculty of Science, Universiti Teknologi Malaysia, 81310 Johor Bahru, Johor, Malaysia
*Corresponding author: nurulaini.jaafar@utm.my

Abstract
The main objective of the research is to investigate the solute dispersion in Casson blood circulation through a stenosed artery with rigid permeable wall. Blood is modelled as a Casson fluid. The study formulates the Casson fluid model for a circular straight pipe where the constitutive and momentum equations are solved to determine fluid velocity. By using the Generalized Dispersion Model (GDM), the convective diffusion equation is solved analytically to obtain dispersion function, mean concentration and concentration. Both steady and unsteady dispersion functions are investigated to provide a comprehensive understanding of solute behaviour. Increased wall permeability improves solute dispersion in the arterial core while decreasing it close to the walls, which lowers flow resistance and improves solute transport. The effects of permeability on the solute dispersion in hemodynamic is analyzed and particularly relevant in altering the flow dynamics with the presence of stenosis and stenosis height on the blood velocity, for example in atherosclerosis. Contrarily, larger stenosis heights result in greater flow resistance and lower central peak velocities but greater central dispersion, which suggests a more turbulent and mixed core flow.

Keywords: Permeability; Casson Fluid; Non-Newtonian; Generalized Dispersion Model; Stenosed Artery

Introduction

Atherosclerosis affects the blood vessels, causing low-density lipoproteins (LDLs) and cholesterol to build up in the inner walls, forming plaques that thicken and stiffen the vessel walls. This constriction hinders hemodynamics to organs and can lead to total obstruction. Blood coagulation issues increase the risk of thrombosis and ischemic damage.[1] Understanding mathematical modeling of hemodynamics, especially using the Casson fluid model, is crucial. Blair [2] and Iida [3] state that Casson and Herschel-Bulkley fluid models investigate arterial porosity. Casson fluid is preferred for cardiovascular research due to its simplicity and effectiveness.

Considering slip at vessel wall, Bigyani and Batra [4] examined an arteriosclerotic artery with a hard permeable wall for its consistent, laminar, and fully developed hemodynamics. Representing blood, they utilized a Casson fluid model and investigated how yield stress affected hemodynamics in arteriosclerotic vessels. For varying arteriosclerotic lesion diameters, they derived the variations of flow resistance, wall shear stress, permeability parameter, slip coefficient, and Casson number. Particularly in larger channels, fluid models including Newtonian fluid model often explain hemodynamics as a homogeneous, incompressible fluid with constant viscosity. Blood behaves, nevertheless, as a non-Newtonian fluid in smaller channels and under different shear rates. Considered variable viscosity that changes exponentially across channel and offers the most correct explanation for reduced shear rates, the Casson fluid model which characterizes hemodynamics through narrow vessels fits Divya *et al.* [5].

Using the Sisko model, Toghraie et al. [6] examined blood as a non-Newtonian fluid under constant heat fluxes directed at the arterial wall. Their work replicated blood as a Newtonian fluid

in a rigid tube, emphasizing blood's non-Newtonian character brought on by changes in shear viscosity resulting from changes in blood cells. Providing insights on hemodynamics transit mechanisms and drug dispersion rates, Rana and Liao [7] examined solute dispersion in non-Newtonian Carreau-Yasuda and Carreau fluids in a straight tube with wall absorption or reaction. They solved non-linear issues with homotopy analysis and the generalized dispersion model. Emphasizing the health hazards of stenosis, Ali *et al.* [8] investigated hemodynamics in stenosed arteries using a mathematical model and the finite difference approach to address the numerical problem.

Investigating the unstable solute dispersion in constant Casson blood circulation via a stenosed artery with inflexible permeable wall is the major objective of this study. The aims are thus to develop the mathematical model of the Casson blood circulation via a stenosed artery with a hard permeable wall. Apart from that, one can solve the momentum and constitutive equations to derive Casson blood circulation velocity over a rigidly permeable wall stenosed artery. Furthermore, integration and Fourier Transform allow one to solve unsteady convective-diffusion equation utilizing Generalized Dispersion Model (GDM) to derive mean concentration of solute, dispersion function, and longitudinal dispersion coefficient. Furthermore, to investigate the solute dispersion in Casson blood circulation via a rigid permeable wall stenosed artery.

Mathematical Formulation

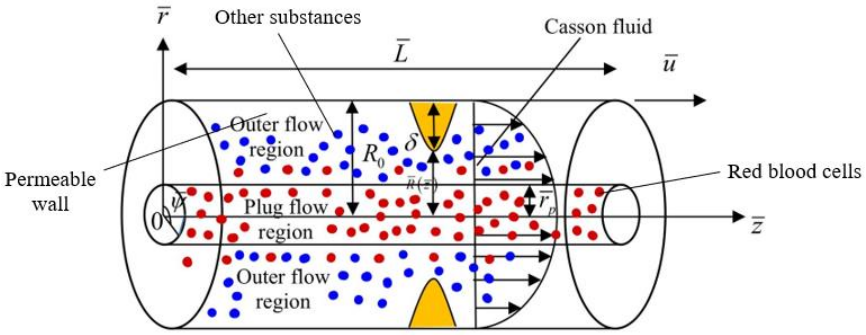

Figure 1 Geometry of pipe flow in the presence of stenosis with permeable wall

Figure 1 depicts the geometry of the arteriosclerotic artery where $\bar{L}$ serves as the length of the conduit, $\bar{u}$ serves as the axial velocity, δ serves as the height of the stenosis, $\bar{R}(\bar{z})$ serves as the stenosed artery, $\bar{R}_0$ serves as the arterial radius in outer flow region of the stenosis, $\bar{\psi}$ serves as the azimuthal angle, $\bar{z}$ serves as the axial coordinate for the circular pipe, and $\bar{r}_p$ serves as the radius of the plug flow region in a circular pipe.

The momentum equation for steady flows is given by

$$\frac{1}{\bar{r}}\frac{d}{d\bar{r}}\left(\bar{r}\bar{\tau}\right)=-\frac{d\bar{p}}{d\bar{z}}, \tag{1}$$

where $\bar{\tau}$ serves as the shear stress and $\bar{p}$ serves as the pressure. The boundary condition of Eqn. (1)is set to be

$$\bar{\tau}=\text{finite at } \bar{r}=0. \tag{2}$$

The Casson fluid model's constitutive equation is given by

$$-\frac{d\bar{u}}{d\bar{r}}=\begin{cases}\dfrac{1}{\bar{k}_c^{\,2}}\left(\sqrt{\bar{\tau}}-\sqrt{\bar{\tau}_y}\right)^2 & \text{if } \bar{\tau}>\bar{\tau}_y,\\ 0 & \text{if } \bar{\tau}\le\bar{\tau}_y,\end{cases} \tag{3}$$

where $\bar{\tau}_y$ serves as the yield stress and $\bar{k}_c$ serves as the viscosity coefficient of Casson fluid. For the unknown velocity $\bar{u}$, the is a slip condition at the wall of the circular pipe and thus the boundary conditions are given by

$$\bar{u}=\bar{u}_B \text{ at } \bar{r}=\bar{R}\left(\bar{z}\right) \tag{4}$$

where the slip velocity $\bar{u}_B$ satisfies the relation

$$\left.\frac{d\bar{u}}{d\bar{r}}\right|_{r=R}=\frac{\bar{\alpha}}{\bar{k}^{1/2}}\left(\bar{u}_B+\frac{\bar{k}}{\bar{k}_c^{\,2}}\frac{d\bar{p}}{d\bar{z}}\right). \tag{5}$$

Here, $\bar{\alpha}$ serves as the slip coefficient, $\bar{k}$ serves as the permeability and $\bar{u}_Q$ serves as the velocity in the porous region. In the arterial wall, a stenosis is assumed to have developed in an axially symmetric manner, which depends upon the axial distance $\bar{z}$ and the height of its growth. In such a case, the arterial radius $\bar{R}\left(\bar{z}\right)$ is given by

$$\bar{R}\left(\bar{z}\right)=\begin{cases}\dfrac{\bar{R}\left(\bar{z}\right)}{\bar{R}_0}=1-\dfrac{\bar{\delta}_h}{2\bar{R}_0}\left(1+\cos\left[\dfrac{2\pi}{\bar{l}_0}\left(\bar{z}-\bar{d}-\dfrac{\bar{l}_0}{2}\right)\right]\right); & \text{for } \bar{d}\le\bar{z}\le\bar{d}+\bar{l}_0\\ =1 & \text{; otherwise}\end{cases} \tag{6}$$

where $\bar{R}\left(\bar{z}\right)$ serves as the radius of the stenosed segment, $\bar{R}_0$ serves as the arterial radius in outer region of stenosis, l_0 serves as the length of stenosis, d being its location and δ_h serves as the maximum height of the stenosis assumed to be much smaller in comparison to the radius, $\bar{R}_0$ of stenosed artery $\bar{\delta}_h\le\bar{R}_0$. The convective-diffusion equation is given by

$$\frac{\partial\bar{C}}{\partial\bar{t}}+\bar{u}\frac{\partial\bar{C}}{\partial\bar{z}}=\bar{D}_m\left(\frac{1}{\bar{r}}\frac{\partial}{\partial\bar{r}}\left(\bar{r}\frac{\partial}{\partial\bar{r}}\right)+\frac{\partial^2}{\partial\bar{z}^2}\right)\bar{C}, \tag{7}$$

where the initial condition is given by

$$\bar{C}\left(\bar{r},\bar{z},0\right)=\begin{cases}\bar{C}_0 \text{ if } \left|\bar{z}\right|\le\dfrac{\bar{z}_s}{2},\\ 0 \quad \text{if } \left|\bar{z}\right|>\dfrac{\bar{z}_s}{2},\end{cases} \tag{8}$$

where $\bar{C}_0$ serves as the reference concentration and $\bar{z}_s$ serves as the length of the solution. As per mentioned above, the boundary condition for a finite level of an axial dispersion according to Gill and Sankarasubramanian [9] is given by

$$\bar{C}\left(\bar{r},\infty,\bar{t}\right)=0, \tag{9}$$

for a symmetry at the circular pipe centre $\bar{r}=0$, the boundary condition is given by

$$\frac{\partial \bar{C}}{\partial \bar{r}}\left(0,\bar{z},\bar{t}\right)=0, \tag{10}$$

while for the solute concentration gradient at the wall $\bar{r}=\bar{R}\left(\bar{z}\right)$, the boundary condition is given by

$$\frac{\partial \bar{C}}{\partial \bar{r}}\left(\bar{R}\left(\bar{z}\right),\bar{z},\bar{t}\right)=0. \tag{11}$$

Dimensionless variables

The dimensionless variables are written as detailed below:

$$\begin{aligned} &C=\frac{\bar{C}}{\bar{C}_0},\ u=\frac{\bar{u}}{\bar{u}_0},\ u_+=\frac{\bar{u}_+}{\bar{u}_0},\ u_-=\frac{\bar{u}_-}{\bar{u}_0},\ u_m=\frac{\bar{u}_m}{\bar{u}_0},\ u_s=\frac{\bar{u}_s}{\bar{u}_0},\ r=\frac{\bar{r}}{\bar{a}},\ r_p=\frac{\bar{r}_p}{\bar{a}},\ \bar{z}=\frac{z\bar{a}^2\bar{u}_0}{\bar{D}_m},\\ &\bar{z}_s=\frac{z_s\bar{a}^2\bar{u}_0}{\bar{D}_m},\ \bar{t}=\frac{t\bar{a}^2}{\bar{D}_m},\ \bar{\tau}=\frac{\tau\bar{k}_c u_0}{\bar{R}_0},\ \bar{\tau}_y=\frac{\tau_y\bar{k}_c u_0}{\bar{R}_0},\ P=-\frac{d\bar{p}}{d\bar{z}},\ P=\frac{\bar{p}}{\bar{k}_c\bar{u}_0}. \end{aligned} \tag{12}$$

where $\bar{u}_0,\ t,\ \tau,\ \tau_y,\ C,\ u,\ u_+,\ u_-,\ u_m,\ u_s,\ r,\ \bar{r}_p,\ z,\ z_s,\ k_c,\ \bar{R}_0,\ P$ are the dimensionless forms of the fluid characteristic velocity, time, shear stress, and yield stress; together with the solute concentration, velocity, mean velocity, outer and plug flow velocity, radial coordinate for circular pipe, plug core radius, axial distance, and solute length, the Casson fluid's viscosity coefficient, the artery's radius in the outer region of stenosis and pressure gradient.

Governing Equation

Substituting Eqn. (12) into Eqn. (1) the dimensionless momentum equation is obtained below

$$\frac{\partial\left(\tau r\right)}{\partial r}=r\left[-\frac{\partial p}{\partial z}\right], \tag{13}$$

where p serves as the pressure, τ serves as the shear stress, z serves as the axial coordinate for circular pipe, r serves as the radial coordinate. The boundary condition of dimensionless momentum equation is given as detailed below:

$$\tau=\text{finite at } r=0. \tag{14}$$

The dimensionless of constitutive equation of Casson fluid is given by

$$-\frac{du}{dr}=\tau+\tau_y-2\sqrt{\tau}\sqrt{\tau_y} \tag{15}$$

where u serves as the dimensionless of Casson fluid velocity, τ_y serves as the dimensionless yield stress and k_c serves as the dimensionless viscosity coefficient of Casson fluid. The boundary conditions are given by

$$u=u_B \text{ at } r=R\left(z\right) \tag{16}$$

The dimensionless of the radius artery in Eqn. (6) is given as detailed below

$$R\left(z\right)=1-\frac{\delta}{2R_0}\left(1+\cos\left[\frac{2\pi}{l_0}\left(z-d-\frac{l_0}{2}\right)\right]\right). \tag{17}$$

Method of Solution

Solving Eqn.(13) and Eqn. (15) using condition in Eqn.(14) and Eqn. (16) respectively, the dimensionless of velocity in the outer non-plug core region is obtained as detailed below:

$$u(r)=\frac{dp}{dz}\left[\frac{r^2-R^2(z)}{4}+\frac{r_p r}{2}-\frac{R(z)r_p}{2}-\frac{2}{3}\sqrt{r_p}\left(r^{\frac{3}{2}}-\left(R(z)\right)^{\frac{3}{2}}\right)\right]+u_B, \tag{18}$$

where dp/dz serves as the dimensionless of axial pressure gradient, C_m serves as the mean concentration of solute across a sectional area of the geometry, r is plug core region, r_p serves as the dimensionless plug flow region, $R(z)$ serves as the dimensionless of radius of the stenosed segment and u_B serves as the dimensionless slip velocity u_B which is given by

$$\left.\frac{du}{dr}\right|_{r=R}=\frac{\alpha}{k^{1/2}}\left(u_B+\frac{k}{k_c^2}\frac{dp}{dz}\right). \tag{19}$$

The dimensionless of velocity of fluid in the plug flow region is given as detailed below:

$$u(r_p)=\frac{dp}{dz}\left[\frac{r_p^2-R^2(z)}{4}+\frac{r_p^2}{2}-\frac{R(z)r_p}{2}-\frac{2}{3}\sqrt{r_p}\left(r_p^{\frac{3}{2}}-\left(R(z)\right)^{\frac{3}{2}}\right)\right]+u_B. \tag{20}$$

The dimensionless mean velocity is given by

$$u_m=\frac{2}{R^2(z)}\left[\frac{dp}{dz}\left[-\frac{\left(R(z)\right)^4}{16}-\frac{\left(R(z)\right)^3 r_p}{12}-\frac{11r_p^{\frac{1}{2}}\left(R(z)\right)^{\frac{7}{2}}}{21}+\frac{r_p^{\,4}}{336}+\frac{r_p^{\frac{5}{2}}\left(R(z)\right)^{\frac{3}{2}}}{3}-\frac{r_p^{\frac{3}{2}}\left(R(z)\right)^{\frac{3}{2}}}{3}\right]+\frac{u_B\left(R(z)\right)^2}{2}\right]. \tag{21}$$

Dimensionless convective-diffusion equation from Eqn. (7) is given by

$$\frac{\partial C}{\partial t}+u\frac{\partial C}{\partial z}=D_m\left(\frac{1}{r}\frac{\partial}{\partial r}\left(r\frac{\partial}{\partial r}\right)+\frac{\partial^2}{\partial z^2}\right)C, \tag{22}$$

To solve Eqn.(22), the approach of Gill and Sankarasubramanian [9], Generalized Dispersion Model (GDM) in terms of derivative series expansion is applied as detailed below:

$$\frac{\partial C_m}{\partial t}(z_1,t)=\sum_{i=1}^{\infty}K_i(t)\frac{\partial^i C_m}{\partial z_1^i}(z_1,t), \tag{23}$$

where $K_i(t)$ represents the transport coefficient. The dispersion function of $f_1(r,t)$ plays an important role in calculating the mean concentration, $C_m(z_1,t)$. The dispersion function is given as detailed below:

$$f_1(r,t)=f_{1s}(r)+f_{1t}(r,t). \tag{24}$$

$f_{1s}(r)$ serves as the dispersion function in the steady state and $f_{1t}(r,t)$ serves as the dispersion function in the unsteady state that describes the time dependent nature of the dispersion of the solute. The differential equation is given by

$$\frac{1}{r}\frac{\partial}{\partial r}\left(r\frac{\partial f_{1s-}}{\partial r}\right)-\left(u\left(r_p\right)-u_m\right)=0 \text{ if } 0\le r\le r_p \tag{25}$$

and the dispersion function in outer region is given by

$$\frac{1}{r}\frac{\partial}{\partial r}\left(r\frac{\partial f_{1s+}}{\partial r}\right)-\left(u\left(r\right)-u_m\right)=0 \text{ if } r_p\le r\le R\left(z\right) \tag{26}$$

Eqn. (25) and Eqn. (26) are solved using Eqn. (26) to get f_{1s_-} and f_{1s_+} as detailed below

$$\frac{\partial f_{1s}}{\partial t}\left(0\right)=0, \tag{27}$$

$$\frac{\partial f_{1s}}{\partial r}R\left(z\right)=0, \tag{28}$$

and

$$\frac{\partial f_{1t}}{\partial r}\left(0,t\right)=0. \tag{29}$$

The steady dispersion function in the plug flow region, f_{1s_-} and outer flow region f_{1s_+} are given as detailed below:

$$f_{1s-}=CI-\frac{1}{48}Ar^2r_p^2+\frac{Ar^2r_p^4}{672R^2\left(z\right)}+\frac{1}{12}Ar^2r_pR\left(z\right)-\frac{2}{21}Ar^2\sqrt{r_p}R^{\frac{3}{2}}\left(z\right)+\frac{1}{32}Ar^2R^2\left(z\right) \tag{30}$$

and

$$\begin{aligned}f_{1s+}=&CI-\frac{1}{68}Ar^4+\frac{8Ar^{\frac{7}{2}}\sqrt{r_p}}{147}-\frac{1}{18}Ar^3r_p-\frac{115}{28224}r_p^4+\frac{Ar^2r_p^4}{672R^2\left(z\right)}+\frac{1}{12}Ar^2r_pR\left(z\right)\\&-\frac{2}{21}Ar^2\sqrt{r_p}R^{\frac{3}{2}}\left(z\right)+\frac{1}{32}Ar^2R^2\left(z\right)-\frac{1}{336}Ar_p^4\log\left(r\right)+\frac{1}{336}Ar_p^4\log\left(r_p\right),\end{aligned} \tag{31}$$

where $A=\left(F\left(t\right)+BP\right)/B$ and $P=dp/dz$ and

$$CI=A\left(\frac{13r_p^4}{7056}+\frac{r_p^6}{5280R^2\left(z\right)}-\frac{7r_pR^3\left(z\right)}{360}+\frac{15\sqrt{r_p}R^{\frac{7}{2}}\left(z\right)}{539}-\frac{R^4\left(z\right)}{96}-\frac{r_p^4}{336}\log\left(r_p\right)+\frac{1}{336}r_p^4\log\left(R\left(z\right)\right)\right). \tag{32}$$

The general solution of $f_{1t}\left(r,t\right)$ is given as

$$f_{1t}\left(r,t\right)=\sum_{m=1}^{\infty}\left(-\frac{2}{J_0^2\left(\lambda_m\right)}\int_0^{R(z)}J_0\left(\lambda_mr\right)f_{1s}\left(r\right)rdr\right)e^{-\lambda_m^2t}J_0\left(\lambda_mr\right). \tag{33}$$

Inverse Fourier Transform (IFT) yields the solution of mean concentration of solute $C_m(z_1,t)$ Iida [3]

$$C_m(z_1,t)=\frac{1}{2}\left[erf\left(\frac{\frac{z_s}{2-z_1}}{2\sqrt{\xi}}\right)+erf\left(\frac{\frac{z_s}{2+z_1}}{2\sqrt{\xi}}\right)\right]. \tag{34}$$

The local concentration $C(r,z_1,t)$ is produced by the following substitutions (ignoring the higher order terms) of $C_m(z_1,t)$ and $f_1(r,t)$. It is given as detailed below

$$C(r,z_1,t)=C_m(z_1,t)+f_1(r,t)\frac{\partial C_m}{\partial z_1}(z_1,t). \tag{35}$$

Results and Discussion

Velocity of the Blood Flow

This section addresses the anticipated outcomes, including the increasing and decreasing of the velocity, steady dispersion function, unsteady dispersion function, and dispersion function with the effect of the permeability, height of the stenosis, radius of the plug flow region in a circular pipe, arterial radius in outer flow region of the stenosis and viscosity coefficient of Casson fluid.

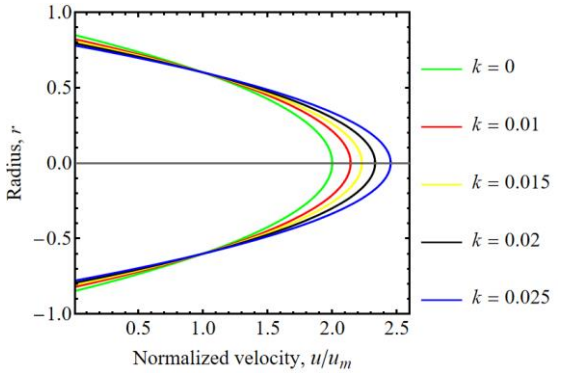

Figure 2: Variation of normalized velocity, u for different values of permeability, k with $k_c=1,\ \mu=1,\ dp/dz=-4,\ r_p=0,\ \delta=0.2, R_0=1,$ $a=0.2,\ l_0=3,\ d=2,$ and $z=4$.

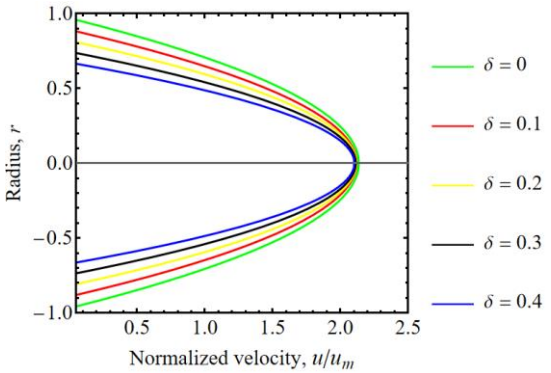

Figure 3: Variation of normalized velocity, u for different height of the stenosis, δ with $k=0.01,\ k_c=1,\ \mu=1,\ dp/dz=-4,\ r_p=0, R_0=1,$ $a=0.2,\ l_0=3,\ d=2,$ and $z=4$.

Figure 2 depicts the variation of normalized velocity, u for different values of permeability, k with $k_c=1,\ \mu=1,\ dp/dz=-4,\ r_p=0,\ \delta=0.2,\ R_0=1,\ a=0.2,\ l_0=3,\ d=2,$ and $z=4$. As permeability escalates, the normalized velocity at the arterial core escalates. Higher permeability leads to decreased normalized velocity near the artery wall. Increased permeability allows more fluid to pass through the artery wall, reducing the overall flow resistance. This increase in resistance increases the peak normalized velocity at the centre because the fluid spreads more evenly throughout the artery.

Figure 3 depicts the variation of normalized velocity, u for different height of the stenosis, δ with $k=0.01,\ k_c=1,\ \mu=1,\ dp/dz=-4,\ r_p=0,\ R_0=1,\ a=0.2,\ l_0=3,\ d=2,$ and $z=4$. As the height of the

stenosis escalates, the normalized velocity reduces. This means higher stenosis heights lead to lower peak normalized velocities and a steeper decrease in normalized velocity away from the centre. Higher stenosis heights increase flow resistance, which reduces the overall fluid normalized velocity and results in lower peak normalized velocities.

Steady Dispersion Function of Solute

Figure 4 depicts the variation of steady dispersion function for different values of permeability, k in the hemodynamics with $dp/dz = -4,\ \delta = 0.2,\ r_p = 0.001,\ R_0 = 1,\ l_0 = 3,\ d = 2,\ z = 4,$ and $k_c = 1$. As permeability escalates, the dispersion at the arterial core reduces, while the dispersion near the wall reduces. This means higher permeability results in lower dispersion at the centre and lower dispersion near the wall. The sharp peak in the graph indicates a significant change in dispersion at the centre due to increased permeability. This peak occurs because higher permeability allows more fluid to pass through the artery wall, causing a marked increase in dispersion at the centre compared to the outer regions. The steep change at the centre reflects the significant impact of permeability on the fluid's dispersion behaviour in this region.

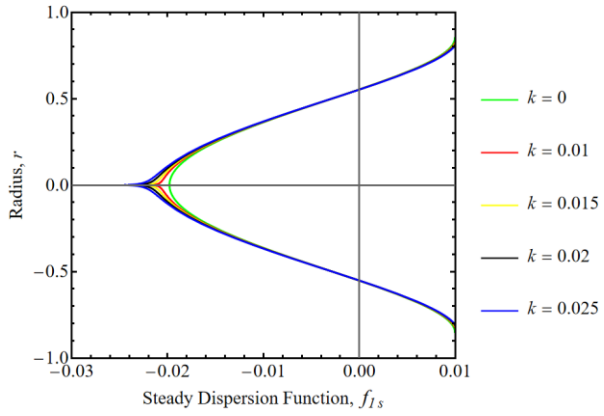

Figure 4: Variation of steady dispersion function for different values of permeability, k in the hemodynamics with $dp/dz = -4,\ \delta = 0.2,\ r_p = 0.001,\ R_0 = 1,\ l_0 = 3,\ d = 2,\ z = 4,$ and $k_c = 1$.

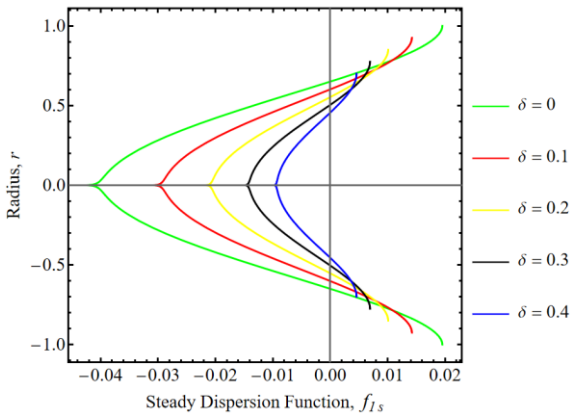

Figure 5: Variation of steady dispersion function for different values of height of the stenosis at the middle point, δ in the hemodynamics with $dp/dz = -4,\ r_p = 0.001,\ R_0 = 1,\ l_0 = 3,\ d = 2,\ z = 4,\ k_c = 1,$ and $k = 0.01$.

Figure 5 depicts the variation of steady dispersion function for different values of height of the stenosis at the middle point, δ in the hemodynamics with $dp/dz = -4,\ r_p = 0.001,\ R_0 = 1,\ l_0 = 3,\ d = 2,\ z = 4,\ k_c = 1,$ and $k = 0.01$. As the height of the stenosis escalates, the dispersion at the arterial core escalates, while the dispersion near the wall reduces. This means higher stenosis heights result in higher dispersion at the centre and lower dispersion near the wall. The sharp peak at the centre of the hemodynamics indicates a significant change in dispersion due to the stenosis. The presence of a permeable wall allows more fluid to pass through, causing a marked increase in dispersion at the centre compared to the outer regions. This steep change at the centre reflects the significant impact of stenosis height on the fluid's dispersion behaviour in this region.

Unsteady Dispersion Function of Solute

Figure 6 depicts the variation of unsteady dispersion function for different values of permeability, k in the hemodynamics with $dp/dz = -4,\ \delta = 0.2,\ r_p = 0.001,\ t = 0.1,\ b = 1,\ R_0 = 1,\ l_0 = 3,\ d = 2,\ z = 4,$ and $k_c = 1$. As permeability escalates, the unsteady solute dispersion at the arterial core escalates slightly.

Conversely, the unsteady solute dispersion near the wall also escalates but to a lesser extent. This means that higher permeability results in higher unsteady solute dispersion both at the centre and near the wall, although the increase is more significant at the centre. It means that the increase in unsteady solute dispersion is greater or more evident at the arterial core compared to the increase near the wall.

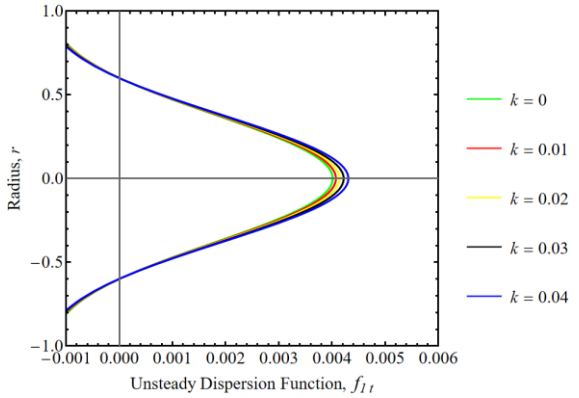

Figure 6: Variation of unsteady dispersion function, f_{1t} for different values of permeability, k in the hemodynamics with $dp/dz = -4$, $\delta = 0.2$, $r_p = 0.001$, $t = 0.1$, $b = 1$, $R_0 = 1$, $l_0 = 3$, $d = 2$, $z = 4$, and $k_c = 1$.

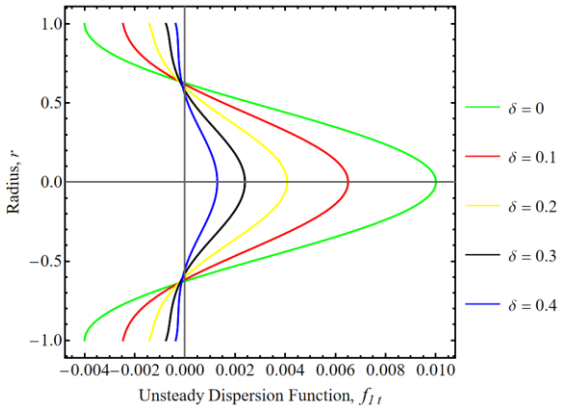

Figure 7: Variation of unsteady dispersion function, f_{1t} for different values of height of the stenosis at the middle point, δ in the hemodynamics with $dp/dz = -4$, $r_p = 0.001$, $b = 1$, $R_0 = 1$, $l_0 = 3$, $d = 2$, $z = 4$, $k = 0.01$, and $k_c = 1$.

Figure 7 depicts the variation of unsteady dispersion function for different values of height of the stenosis at the middle point, δ in the hemodynamics with $dp/dz = -4$, $r_p = 0.001$, $b = 1$, $t = 0.1$, $R_0 = 1$, $l_0 = 3$, $d = 2$, $z = 4$, $k = 0.01$, and $k_c = 1$. As the height of the stenosis escalates, the unsteady solute dispersion at the arterial core reduces. Conversely, the unsteady solute dispersion near the wall escalates. This means that higher stenosis heights result in lower dispersion at the centre and higher dispersion near the wall which can impact the effectiveness of solute transport and potential drug delivery systems within the artery. The decrease in unsteady solute dispersion at the centre with higher stenosis heights implies that the stenosis causes lower mixing and turbulence in the central region of the hemodynamics. Conversely, the increase in dispersion near the wall suggests that the stenosis stabilizes the flow in the peripheral regions, increasing mixing. Overall, higher stenosis heights lead to more significant disruption and mixing in the central flow while making the outer flow regions more stable.

Dispersion Function of Solute

Figure 8 depicts the dispersion function variation for different values of permeability, k in the hemodynamics with $dp/dz = -4$, $\delta = 0.2$, $r_p = 0.001$, $t = 0.1$, $b = 1$, $R_0 = 1$, $l_0 = 3$, $d = 2$, $z = 4$, and $k_c = 1$. As the permeability escalates, the dispersion function reduces at the centre, and escalates near the artery wall, implying that solute dispersion is reduced in the central region and enhanced at the boundaries. This suggests that a permeable wall allows less solutes to disperse into the centre of the hemodynamics, leading to a concentrated dispersion at the centre and a higher concentration near the vessel wall. At the arterial core, there is a sharp peak in the dispersion function, indicating a higher concentration of solutes when permeability is present due to the significant concentration gradient created by the initial dispersion from the centre outward. This implies that with increased permeability, solutes are more effectively transported.

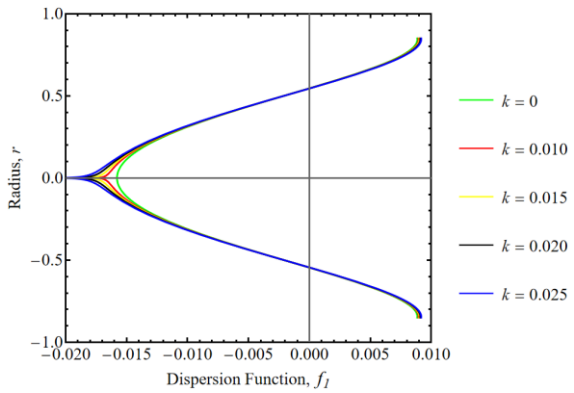

Figure 8: Dispersion function variation, f_1 for different values of permeability, k in the hemodynamics with $dp/dz = -4,\ \delta = 0.2,$ $r_p = 0.001,\ t = 0.1,\ b = 1,\ R_0 = 1,\ l_0 = 3,\ d = 2,\ z = 4,$ and $k_c = 1$.

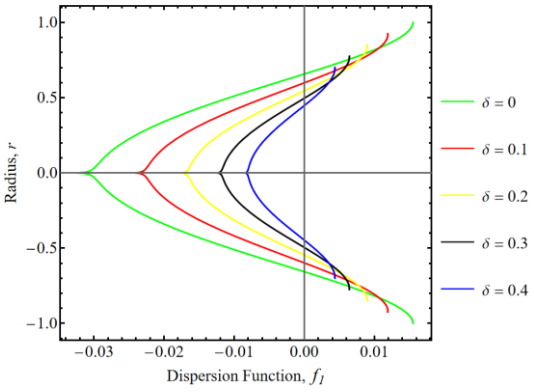

Figure 9: Dispersion function variation, f_1 for different values of the height of stenosis at the middle point, δ in the hemodynamics with $dp/dz = -4,\ r_p = 0.001,\ t = 0.1,\ b = 1, R_0 = 1,$ $l_0 = 3,\ d = 2,\ z = 4,\ k = 0.01,$ and $k_c = 1$.

Figure 9 depicts the dispersion function variation for different values of the height of stenosis at the middle point, δ in the hemodynamics with $dp/dz = -4,\ r_p = 0.001,\ t = 0.1,\ b = 1,\ R_0 = 1,$ $l_0 = 3,\ d = 2,\ z = 4,\ k = 0.01,$ and $k_c = 1$. As the height of the stenosis escalates, the dispersion function at the arterial core escalates, while the dispersion function near the wall reduces. This implies that higher stenosis stabilizes the central flow with reduced dispersion, leading to lower central blood normalized velocity, while increasing mixing and turbulence in the peripheral regions, resulting in higher blood normalized velocity near the wall. The sharp peak at the centre indicates significant changes in dispersion due to the presence of a permeable wall, which allows more fluid to pass through, increasing central mixing and turbulence compared to the outer regions. This suggests that the stenosis and permeability collectively enhance central dispersion and stabilize outer flow.

Conclusion

The study concludes that the solute dispersion in Casson blood circulation through a stenosed artery with a rigid permeable wall is significantly influenced by key parameters such as permeability and the height of the stenosis. The findings reveal that increased wall permeability enhances solute dispersion at the artery's centre, while reducing it near the walls, thereby lowering flow resistance and facilitating better solute transport. Higher stenosis heights, on the other hand, increase flow resistance, leading to lower central peak velocities but higher dispersion at the centre, indicating a more turbulent and mixed central flow. These insights into the dynamics of solute dispersion under varying conditions of permeability and stenosis provide valuable implications for designing more effective medical interventions and drug delivery systems targeting arterial diseases.

References

[1] Izzatillo qizi, T.J. & Farhod o‘g‘li, S.F. (2022) Atherosclerosis: Causes, symptoms, diagnosis, treatment and prevention, Zenodo. Available at: https://doi.org/10.5281/zenodo.6988810

[2] Blair G. W. (1959). An equation for the blood circulation, plasma and serum through glass capillaries. Nature, 183(4661), 613–614. https://doi.org/10.1038/183613a0

[3] Iida. (1978). Influence of plasma layer on steady hemodynamics in microvessels, Jpn. J. Appl. Phys. 17 203–214.

[4] Bigyani, D. & Batra, R.L. (1995) non-Newtonian blood circulation in an arteriosclerotic blood vessel with rigid permeable wall, Journal of Theoretical Biology. https://www.sciencedirect.com/science/article/pii/S0022519385701154

[5] B.B. Divya, G. Manjunatha, C. Rajashekhar, Hanumesh Vaidya & K.V. Prasad (2021). Analysis of temperature dependent properties of a peristaltic MHD flow in a non-uniform channel: A Casson fluid model, Ain Shams Engineering Journal, Volume 12, Issue 2, Pages 2181-2191, ISSN 2090-4479, https://doi.org/10.1016/j.asej.2020.11.010.

[6] Toghraie, D., Esfahani, N. N., Zarringhalam, M., Shirani, N., & Rostami, S. (2020). Hemodynamics analysis inside different arteries using non-newtonian sisko model for application in Biomedical Engineering. Computer Methods and Programs in Biomedicine, 190, 105338. https://doi.org/10.1016/j.cmpb.2020.105338

[7] Rana, J., & Liao, S. (2019). A general analytical approach to study solute dispersion in non-Newtonian fluid flow. European Journal of Mechanics-B/Fluids, 77, 183-200.

[8] Ali, A., Hussain & M., Anwar, M.S. (2021) Mathematical modeling and parametric investigation of hemodynamics through a stenosis artery. Appl. Math. Mech.-Engl. Ed. 42, 1675–1684. https://doi.org/10.1007/s10483-021-2791-8

[9] Gill, W. N., & Sankarasubramanian, R. (1970). Exact analysis of unsteady convective diffusion. Proceedings of the Royal Society of London. A. Mathematical and Physical Sciences, 316(1526), 341–350. https://doi.org/10.1098/rspa.1970.0083